Available online at www.sciencedirect.com
SCIENCE DIRECT®
Carbohydrate Research 340 (2005) 2550–2557
Carbohydrate RESEARCH

The α-(1→6) glycosidic linkage as a novel conformational entropic regulator in osmoregulated periplasmic α-cyclosophorohexadecaose

Youngjin Choi[a] and Seunho Jung[a,b,*]

[a]*Department of Microbial Engineering, Bio/Molecular Informatics Center, Konkuk University, 1 Hwayang-dong, Gwangjin-gu, Seoul 143-701, South Korea*
[b]*Department of Advanced Technology Fusion, Bio/Molecular Informatics Center, Konkuk University, Seoul 143-701, South Korea*

Received 27 May 2005; received in revised form 27 August 2005; accepted 31 August 2005
Available online 5 October 2005

Abstract—Molecular dynamics simulations were performed to explain the conformational effect of an α-(1→6)-glycosidic linkage upon the cyclic osmoregulated periplasmic glucan (OPG) produced by *Xanthomonas campestris* pv. *citri*. We suggest that a single α-(1→6)-glycosidic linkage in cyclic OPG functions as a novel entropic regulator, which reduces the conformational entropy of cyclic OPG and increases the motional entropy of solvent water molecules.

Keywords: Biological water; Conformational entropy; Glycosidic linkage; Molecular dynamics; Cyclic osmoregulated periplasmic glucan

1. Introduction

Molecular order–disordering or conformational entropy is an essential determinant in the physiochemical properties of macromolecules. Protein engineers use an entropic regulation technique with proline insertion at the second site of β-turns or at the '*N*-cap' position of a α-helix to increase protein thermostability by reducing the conformational entropy of unfolding.[1] In lipid molecules, conformational entropy is regulated by the degree of chain unsaturation or the introduction of a macrocyclic ring structure.[2] However, the study of carbohydrates with regard to their folding structure and conformational properties has not been well investigated.

In this paper, we investigated the α-(1→6)-glycosidic linkage as a conformational entropic regulator in a microbial cyclooligosaccharide, which is a type of cell-associated osmoregulated periplasmic glucan (OPG). OPGs are known to be involved in microbe–plant interactions in both pathogenesis and symbiosis.[3] The conformational analysis of cyclic OPGs is a challenging problem due to the high flexibility of the glycosidic linkages.[4] The rapid conformational interconversion and the resulting magnetic equivalence of the glucosidic residues of the OPGs make it experimentally difficult to distinguish the interactions of individual residues. Recent studies on OPG revealed that *Xanthomonas campestris* pv. *citri* synthesizes a neutral cyclic OPG (α-cyclosophorohexadecaose) containing 16 glucose residues linked by β-(1→2)-glycosidic bonds and one α-(1→6)-glycosidic bond.[5] The presence of a single α-(1→6) linkage was known to make ring closure feasible and induce structural constraints in the cyclic OPG. Such constraints may significantly simplify the conformational analysis of this cyclic OPG and may also endow them with unique physical properties.[6] However, the effect of the α-(1→6)-glycosidic bond upon the conformation or the solvation of the cyclic OPG has not been investigated in detail.

* Corresponding author. Tel.: +82 2 450 3520; fax: +82 2 452 3611; e-mail: shjung@konkuk.ac.kr

0008-6215/$ - see front matter © 2005 Elsevier Ltd. All rights reserved.
doi:10.1016/j.carres.2005.08.020

In this study, we conducted comparative molecular modeling studies to elucidate the effect of structural constraints induced by the presence of one α-(1→6)-glycosidic bond in α-cyclosophorohexadecaose (**XAN16**). We also carried out a similar study on a hypothetical cyclic OPG (**CYS16**) containing D-glucopyranose residues, which has the same molecular weight as **XAN16**, but in which all of the linkages are β-(1→2). We performed molecular dynamics (MD) simulations on the aforementioned two cyclic OPGs. Our goals were to determine, through the use of MD simulations, if a specific linkage pattern can serve as an entropic regulator in carbohydrate folding and to clarify the relationship between the conformational entropy of the carbohydrate molecules and biological function at an atomic level.

2. Computational methods

Molecular models for **XAN16** and **CYS16** were built with the InsightII/Biopolymer program (version 2000, Accelrys Inc. San Diego, USA). The β-(1→2) glycosidic linkage in both cyclic OPGs is described by two dihedral angles: Φ = H-1–C-1–O-1–C-2′ and Ψ = C-1–O-1–C-2′–H-2′, while the α-(1→6) linkage in **XAN16** is described by three dihedral angles: Φ' = H-1–C-1–O-1–C-6′, Ψ' = C-1–O-1–C-6′–C-5′ and Ω = O-1–C-6′–C-5′–H-5′ (Fig. 1).

The initial coordinates of **XAN16** and **CYS16** were determined using simulated annealing molecular dynamics (SA-MD), because their three-dimensional structures have not been identified. SA-MD simulations were performed using the CHARMM 28b2 program[7] with the parm22 sugar parameter set. In these simulations, the temperature was varied between 300 and 1000 K 60 times. The total time for SA-MD simulation was 30 ns. Ten structures were saved and fully energy minimized at the end of each production phase at 300 K, and the lowest-energy conformation among the 10 structures was selected for the initial structure of the subsequent SA-MD cycle. Stereodiagrams of the SA-MD conformations of **XAN16** and **CYS16** with the lowest energy, which are similar to each other, are shown in Figure 2. The starting configurations of each cyclic OPG for the MD simulations in water were taken from the SA-MD conformations with the lowest-energy value. The geometries of these molecular models were fully optimized before each MD run. A TIP3P three-site rigid water[8] model was used to solvate **XAN16** and **CYS16**. Water molecules were removed if they were closer than 2.6 Å to any heavy atoms of the cyclic OPG. Each system was constructed using periodic boundary conditions in a 40 Å × 40 Å × 40 Å box, consisting of **XAN16** and 1607 water or **CYS16** and 1605 water molecules. The system was minimized by 1000 steps of conjugate gradient, followed by Adopted Basis Newton–Raphson minimization until the root-mean-square gradient was less than 0.001 kcal/mol. The MD simulations were performed using the CHARMM 28b2 program in the isothermal–isobaric ensemble (P = 1 bar, T = 298 K). The particle mesh Ewald (PME) summation method[9] was used to

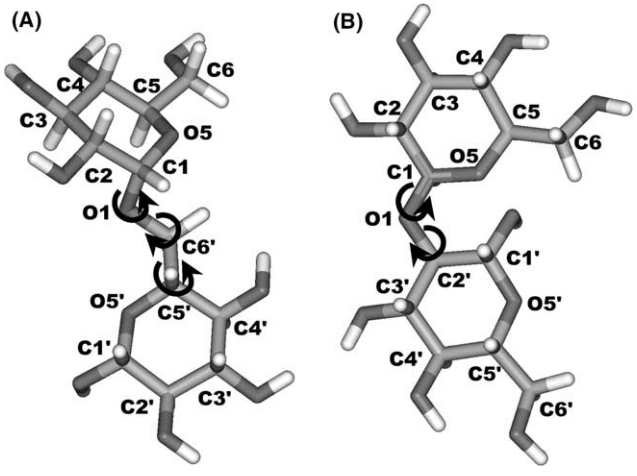

Figure 1. Schematic diagrams of the glycosidic linkage of α-(1→6) linked glucan (A) and β-(1→2) linked glucan (B) including atomic labels. Each glycosidic dihedral angle is marked with arrows. An α-(1→6) linkage has additional glycosidic dihedral angle compared to a β-(1→2) linkage.

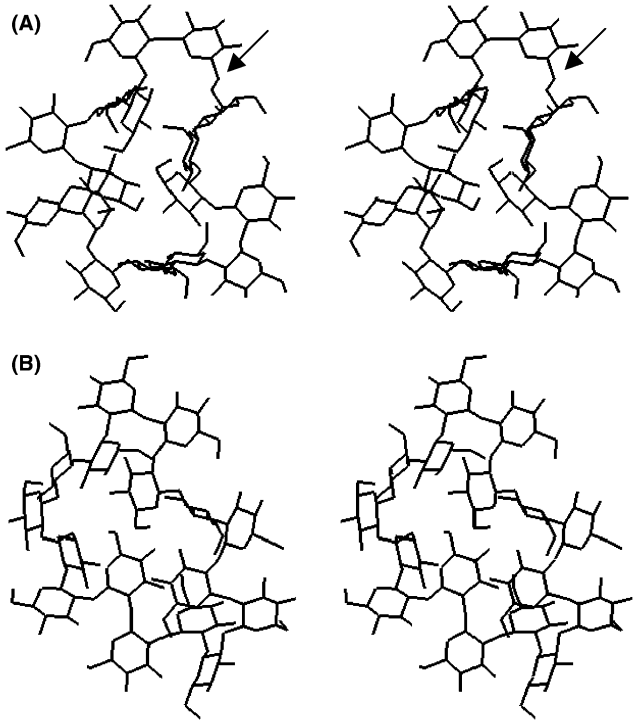

Figure 2. Stereoview of the lowest energy structure computed by SA-MD simulations for the **XAN16** (A) and **CYS16** (B) conformations. An arrow indicates the α-(1→6)-linked glycosidic bond in **XAN16**. Hydrogen atoms are omitted for clarity.

treat long-range electrostatic interactions. The bond lengths of water molecules were constrained with the SHAKE algorithm.[10] The time step was 1.0 fs and the non-bonded pair list was updated every 50 steps. Short-range non-bonded interactions were truncated with a 13 Å cutoff. The temperature and pressure of the system was regulated using the Langevin piston method in conjunction with Hoover's thermostat.[11] The system was gradually heated to 298 K for 20 ps and equilibrated for 100 ps at this temperature. The produced MD trajectory with one snapshot per 1.0 ps was collected for 1 ns. The vibrational entropies for conformational changes of the **XAN16** or **CYS16** were analyzed using the normal modes analysis facility (Vibran module) of the CHARMM program.

3. Results and discussion

3.1. Conformational and hydrational properties of the cyclic OPGs

The stable solution conformations for **XAN16** and **CYS16** were traced with 1 ns molecular dynamics simulations using the CHARMM program. The 1 ns MD simulations with PME electrostatics were long enough for estimation of thermodynamic properties or molecular conformation.[12] Comparison of the individual simulations provide insight into aspects of the conformational differences between **XAN16** and **CYS16**. Because the X-ray crystallographic structure for **XAN16** has not been reported, we estimated the interglycosidic proton–proton distances by comparing our computational model with York's observations[6a] obtained from NMR spectroscopy. In these studies, strong H-1–H-2′ NOE interactions were observed for every β-(1→2) glycosidic bond of **XAN16** while H-1–H-1′ or H-2–H-2′ cross-peaks did not appear.[6a] In our MD simulations, **XAN16** showed a closer interproton distance for H-1–H-2′ (2.3 Å) than the average distances of H-1–H-1′ (4.1 Å) or H-2–H-2′ (4.3 Å), in agreement with York's NMR investigations (Table 1).

To gain further insight into the differences between **XAN16** and **CYS16**, we analyzed their conformational changes during the MD simulations. All glycosidic dihedral angles (Φ,Ψ) of **XAN16** and **CYS16** were populated in the $-70°$ to $+70°$ region, with average values of $\Phi = 26.2°$, $\Psi = 3.1°$ (**XAN16**) and $\Phi = 25.8°$, $\Psi = 2.8°$ (**CYS16**). These values are in close agreement with previous reports on the conformational analysis of β-sophorose,[13] a β-(1→2)-linked disaccharide. Distinct differences in glycosidic dihedral angles between **XAN16** and **CYS16** were not observed. We computed root-mean-square fluctuation (RMSF) values for the atomic coordinates of each glucopyranose residue of cyclic OPG during the MD simulations. The calculated

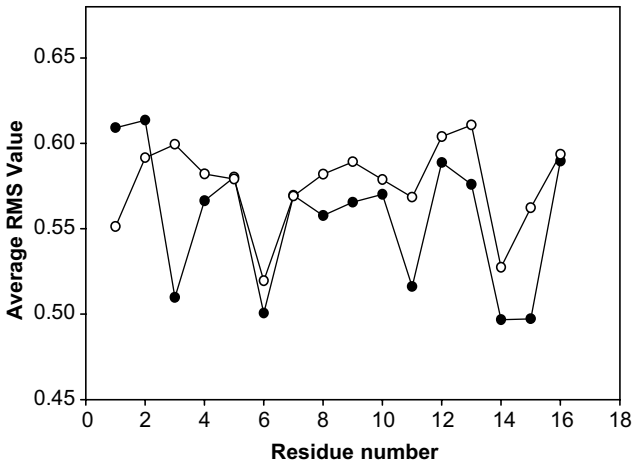

Figure 3. Average RMS fluctuations for the each glucopyranose ring of **XAN16** (●) and **CYS16** (○) during the MD simulations.

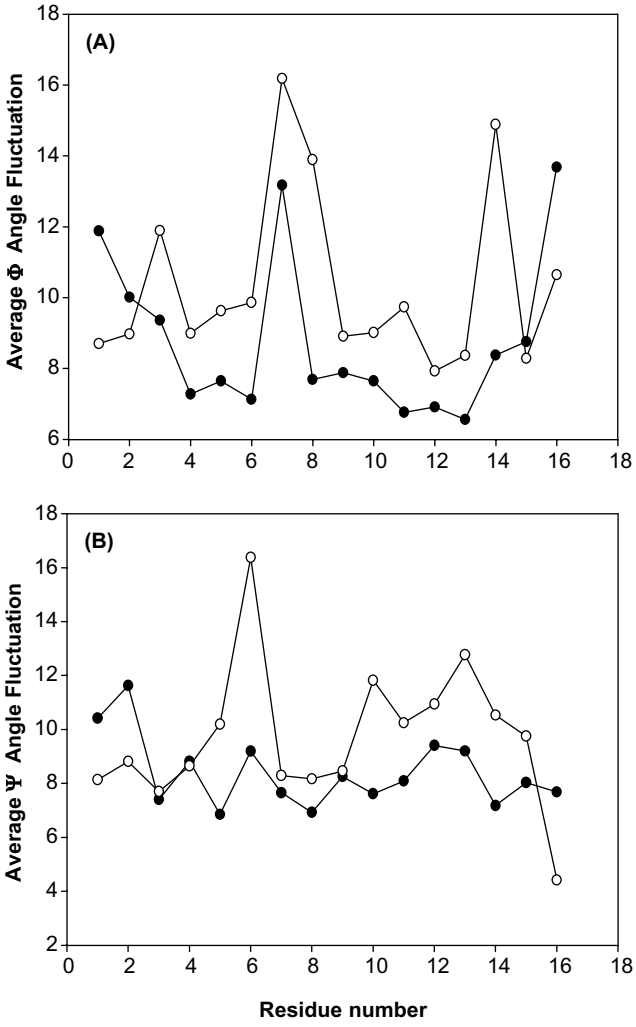

Figure 4. The conformational properties of **XAN16** (●) and **CYS16** (○). (A) Average Φ dihedral fluctuation for each glycosidic linkage during the MD simulations. (B) Average Ψ dihedral fluctuation for the each glycosidic linkage during the MD simulations.

average RMSF values were 0.558 for **XAN16** and 0.577 for **CYS16** (Fig. 3), demonstrating that each residue of **CYS16** was more fluxional during the MD simulations compared with those in **XAN16**. A distinct difference between **XAN16** and **CYS16** was observed with regard to dihedral angle fluctuations (Fig. 4) as a function of the glycosidic bond position relative to the α-(1→6)-linkage. Rotational motions about dihedral angles affect the chemical shift and the vicinal coupling constants in NMR spectrum.[14] The alternating pattern of dihedral angle fluctuations observed in Figure 4 is consistent with a previous study of NMR experiments[6] for a cyclic OPG containing an α-(1→6)-linkage. A large change in Φ and a smaller change in Ψ indicate that cyclic OPG are constrained by the *exo*-anomeric effect.[15] These results indicate that our solution conformation model for **XAN16** is reasonable in comparison with that determined by NMR spectroscopy. This good agreement suggests that the force field and the computational methods employed here are adequate for the molecular dynamics studies of **XAN16** and **CYS16**.

The overall average value of Φ dihedral fluctuation is 8.79 for **XAN16** and 10.36 for **CYS16**, while for Ψ the average dihedral fluctuation is 8.39 for **XAN16** and 9.70 for **CYS16**. This means that the individual anomeric proton resonances in NMR spectrum of **XAN16** can be distinguished due to small fluctuations and slow interconversions of glycosidic bonds in **XAN16**. The conformational rigidity of **XAN16** was also confirmed by the solvent-accessible surface area[16] (SASA) changes during MD simulations (Fig. 5). **XAN16** showed stable SASA changes with small fluctuations. In contrast, the fluctuation for the SASA of **CYS16** was quite large during the MD simulations. Overall, the results of the MD simulations showed the enhanced rigidity of the cyclic OPG containing an α-(1→6)-glycosidic linkage.

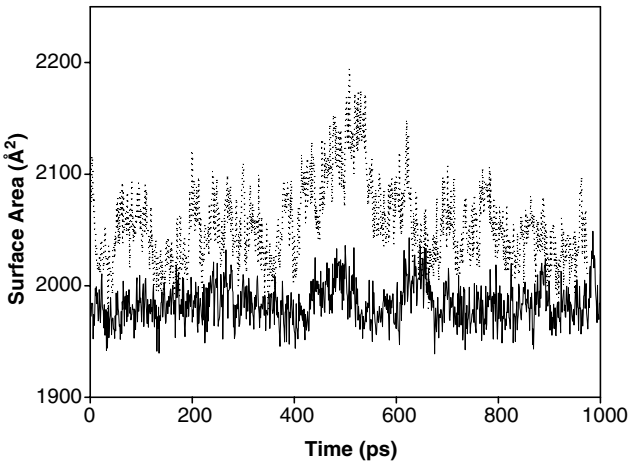

Figure 5. Solvent-accessible surface area changes of each cyclic glucan during the MD simulations. The **XAN16** (solid line) shows compact and stiff conformational characteristics compared to **CYS16** (dashed line).

We investigated solute–solvent interactions to establish the origin of the low dihedral and SASA fluctuations observed in **XAN16** (Table 2). Water has a strong influence on both the structure and dynamics of carbohydrates in solution, particularly through hydrogen bonding to the hydroxyl groups of the solute. The average number of hydrogen bonds with water was 72.3 for **XAN16** and 77.8 for **CYS16** during MD simulations and the average number of inter-residue hydrogen bonds between the glucopyranose residues was 55.3 for **XAN16** and 51.6 for **CYS16**, respectively. The conformations of both cyclic OPGs were stabilized by hydrogen bonds between the hydrogen of the C-3–OH group and the glycosidic O-1 of the preceding β-D-glucopyranose unit with an inter-atomic distance d[H···O] of 2.74 Å for **XAN16** and 2.80 Å for **CYS16**, respectively.

Table 1. Inter-proton distances between glycosidic bonds of each cyclic OPG

Glycosidic bond	XAN16			CYS16		
	H1–H1′	H1–H2′	H2–H2′	H1–H1′	H1–H2′	H2–H2′
1	4.468	2.225	4.407	4.038	2.017	4.257
2	4.349	2.035	4.356	4.520	2.766	4.337
3	4.503	2.144	4.395	3.517	2.416	3.540
4	4.574	2.793	4.232	4.510	2.202	4.421
5	3.742	2.172	3.806	4.220	2.027	4.313
6	4.447	2.069	4.434	4.479	2.253	4.406
7	4.562	2.386	4.337	4.533	2.379	4.387
8	3.707	2.117	4.041	3.621	2.268	3.845
9	4.552	2.314	4.389	4.544	2.305	4.396
10	4.040	2.006	4.230	4.124	2.021	4.252
11	4.491	2.123	4.396	4.484	2.118	4.400
12	2.111	3.657	4.522	2.107	3.648	4.533
13	4.579	2.352	4.314	4.545	2.357	4.334
14	4.552	2.479	4.377	4.483	2.196	4.411
15	2.330	2.225	3.771	4.538	2.703	4.269
Average	4.067	2.340	4.267	4.151	2.378	4.273

Table 2. Summarized physiochemical properties of cyclic OPG based on results of the MD simulations

Property	XAN16	CYS16
N_{inter_hbond} [a]	72.3	77.8
N_{intra_hbond} [b]	55.3	51.6
$d_{[O1\cdots HO3']}$ [c]	2.74	2.80
$RMS_{glucopyranose}$ [d]	0.558	0.577
N_{HD} [e]	2.558	2.748
D (cm^2/s) [f]	0.50×10^{-5}	0.32×10^{-5}
Surface area ($Å^2$)	1984	2062
Radius of gyration (R_G)	7.92	8.09

[a] Number of hydrogen bonds between cyclic glucan and solvent water molecules.
[b] Number of intramolecular hydrogen bonds of each cyclic glucan.
[c] Average atomic distance of intramolecular hydrogen bond between O-1 and OH-3.
[d] Average root-mean-square fluctuation values for the glucopyranose ring of cyclic glucans.
[e] Average hydration number for a glucopyranose ring of each cyclic glucan.
[f] Diffusion coefficient of solvent water calculated from the mean-square displacement values within a first solvation shell.

These results indicate that **XAN16** prefers making inter-residue hydrogen bonds over the formation of hydrogen bonds with solvent water. Such strong intramolecular hydrogen bonds result in a more constrained three-dimensional structure in **XAN16** compared with the structure of **CYS16**. We also estimated the hydration numbers of the two cyclic OPGs as given by the average number of water molecules in strong interaction with the solute (less than 4.0 Å from the solute oxygens). The dynamic hydration number is an important physical quantity, which describes the hydration characteristics of a solute. The average hydration number per glucopyranose residue is 2.558 for **XAN16** and 2.748 for **CYS16**, respectively.

3.2. Conformational entropy of the cyclic OPGs

The conformational states of **XAN16** and **CYS16** can be described by using the asphericity parameter,[17] which is defined as $\eta = A^3/36\pi V^2$, where A is the surface area and V is the volume for each of **XAN16** and **CYS16**. A perfect sphere takes a value of 1 by definition (because $A = 4\pi r^2$, $V = 4/3\pi r^3$), while a cube has $\eta = 1.91$ and ice has $\eta = 2.25$. This value is apt to decrease when the molecule forms an isotropic shape. The asphericity parameter can give information on molecular shape and conformational degrees of freedom of the cyclic OPGs. The calculated asphericity parameters for the MD trajectories of both **XAN16** and **CYS16** show a Gaussian distribution (Fig. 6). The **CYS16** showed a broad distribution of the asphericity parameter while **XAN16** showed a relatively sharp distribution. That means the **CYS16** has a larger degree of conformational freedom compared to **XAN16**. The calculated vibrational entropy (S_{vib}) from normal mode analysis for

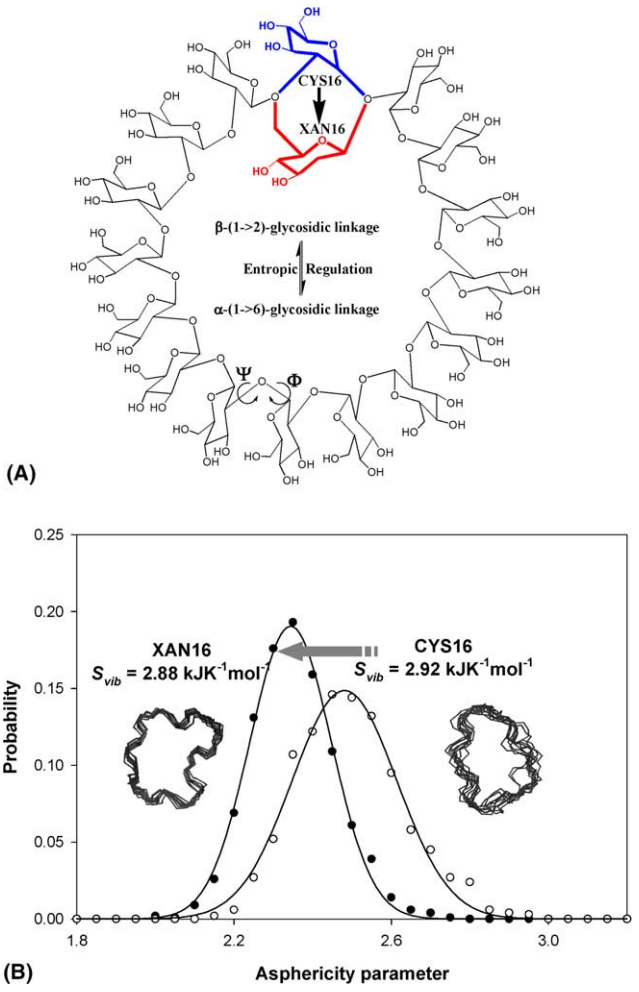

Figure 6. (A) Schematic representations of molecular structure of **XAN16** and **CYS16**. (B) Distributions of asphericity parameter and calculated vibrational entropy for the **XAN16** (●) and **CYS16** (○). Inset pictures are superimposed drawings of **XAN16** and **CYS16** backbones as a series of snapshots at 100-ps intervals in a 1000-ps MD simulations. The calculated entropy change of **CYS16** to **XAN16** is -19.92 kJ mol^{-1} at 298 K; Asphericity parameter $\eta = A^3/36\pi V^2$.

XAN16 was 2.88 kJ/K mol and for **CYS16** was 2.92 kJ/K mol. The $T\Delta S_{vib}$ was calculated to be reduced by 11.92 kJ/mol if **CYS16** is changed to **XAN16** at 298 K. Overall, these results indicate that **CYS16** has various conformational ensembles and therefore higher conformational entropy while **XAN16** is more conformationally restricted and thus lower conformational entropy.

3.3. Rotational motions of the water around cyclic OPGs

The relationship between the conformational entropy of cyclic OPG and rotational motion of water molecules was characterized by radial pair distribution functions (RDF) and the rotational correlation time of water molecules (Fig. 7). The RDF $g(r)$ of **XAN16** has a well-defined first solvation shell with a density

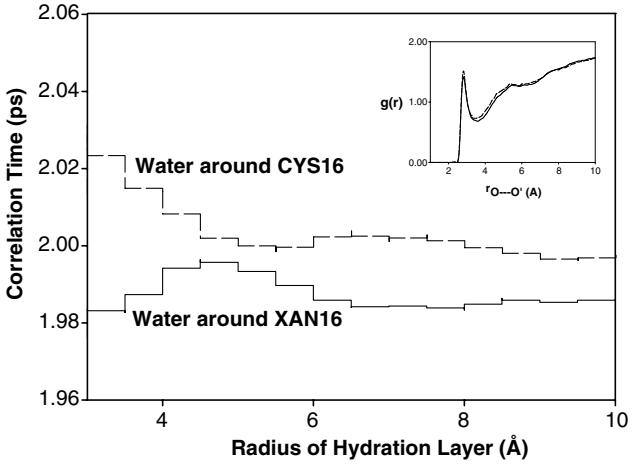

Figure 7. The solute–solvent radial distribution functions (inset) and averaged rotational correlation times for TIP3P water in the vicinity of **XAN16** (solid line) or **CYS16** (dashed line). The RDF was plotted versus distance in Å for the distribution of water oxygen around solute oxygen atoms. The averaged correlation time was plotted versus the distance (Å) of the water molecule from the surface of **XAN16** or **CYS16**.

peak at 2.8 Å and a peak density of about 1.41. Similarly, the RDF calculated for **CYS16** displays a density peak at 2.8 Å and a peak density of about 1.51. Because the radial pair distribution function reflects the interaction with the solvent water molecules, it indicates that during the MD simulations each cyclic OPG was solvated by water at a similar level. To characterize the water structures and to follow the dynamics of solutes involving water, it is necessary to examine the motions of the solvent in detail. Hence, we calculated the rotational correlation times[18] of water molecules for three rotational motions, wagging, twisting, and rocking (τ_{wag}, τ_{twist}, τ_{rock}) from the MD trajectory files. Each rotational correlation time for three motions are plotted in Figure 8. The rotational correlation time was calculated by fitting the exponential decay component of the corresponding time correlation function $C(t)$ to an exponential function of the form $C(t) = Ae^{-t/\tau}$, where τ is the correlation time. The value of each τ_{wag}, τ_{twist}, and τ_{rock} within the first solvation shell was 1.886, 2.578, and 1.487 ps for **XAN16** and 1.913, 2.634, and 1.546 ps for **CYS16**. The average values of the three motions of τ for **XAN16** were smaller than those of **CYS16** in any distance range of solute-solvent (Fig. 8). The smaller τ value of water for **XAN16** indicates that the water around **XAN16** rotates more freely compared to **CYS16**. The RDF and rotational correlation time data suggest that water molecules around the cyclic OPG were positionally restricted but orientationally free to form hydrogen bonds in all directions. These differences in the solvent interaction between **XAN16** and **CYS16** can be explained in terms of molecular curvature. **XAN16** showed higher curvature

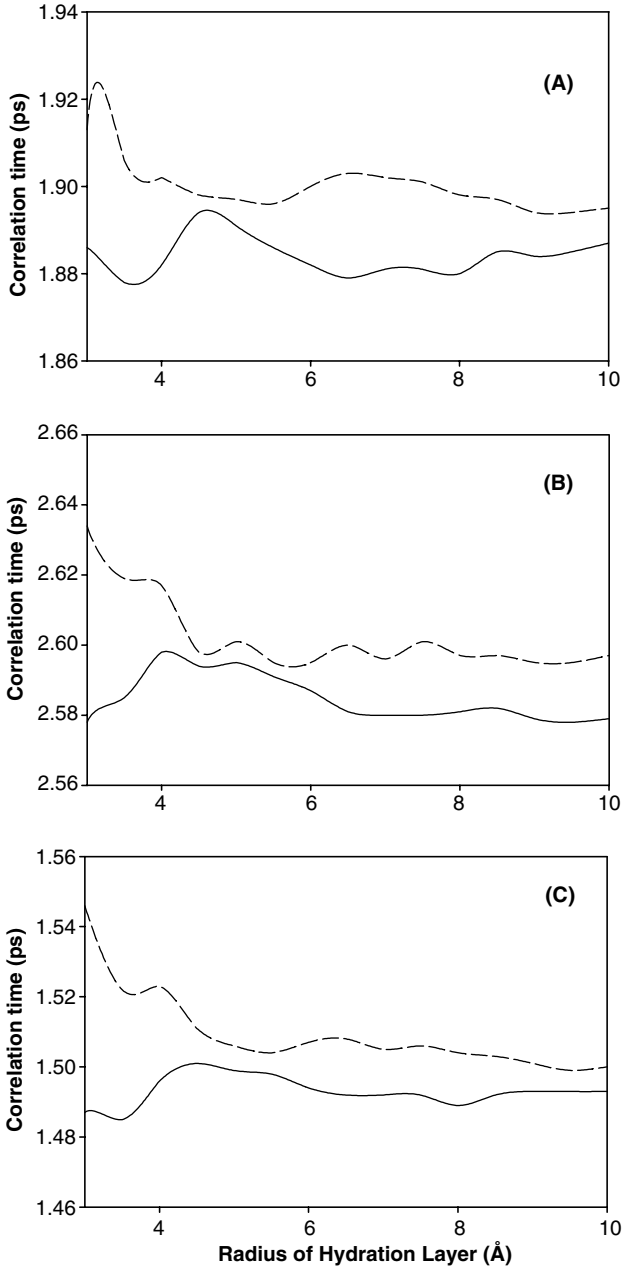

Figure 8. Rotational correlation times for TIP3P water in the vicinity of **XAN16** (solid line) or **CYS16** (dashed line). The three rotational motions, so called wagging (A), twisting (B), and rocking (C) are plotted versus the distance (Å) of the water molecule center of mass from the surface of **XAN16** or **CYS16**.

than **CYS16** as determined by the asphericity parameter values. As the curvature of the solute's surface decreases, water molecules are forced to adopt more restricted orientations to form the maximum number of hydrogen bonds.[19] These results indicate that the greater restricted conformational freedom of **XAN16** enforces a decrease of motional entropy of **XAN16** itself and promotes an increase of rotational entropy of solvent water molecules.

4. Molecular motion of cyclic OPGs and water interaction

The free rotation of water around **XAN16** may be related to the restriction of the global motion of **XAN16**. The global motions of the cyclic glucans were estimated using time correlation functions for the vectorial motion of **XAN16** and **CYS16** (Fig. 9). A molecular vector is defined as a virtual vector that is created by the positions between the glycosidic oxygens of residue **1** and residue **8**. The time correlation function of the motion is defined by the following formula $Q(t) = X_1(t) - X_2(t)$, where $X(t)$ is the time function of the atomic position of glycosidic oxygen of residue **1** (X_1) or residue **8** (X_2). The correlation function provides a measure of the long-time scale motions of overall glucopyranose residues in the cyclic OPGs. The calculated results suggest that **XAN16** has slower motional properties compared with **CYS16**.

Computation of the conformational and hydrational properties of two cyclic OPGs, **XAN16** and **CYS16**, give a picture of the effect of an α-(1→6)-glycosidic linkage upon β-(1→2)-linked cyclic OPG. Dihedral angle fluctuation and solvent-accessible surface area changes were distinct for **XAN16** and **CYS16**. The conformational constraint of **XAN16** was evidenced by the differences in asphericity parameter and vibrational entropy for the **XAN16** and **CYS16**. The conformational characteristics of the cyclic OPGs were correlated with distinct hydration patterns between **XAN16** and **CYS16**. Water molecules are known to play an important role in the regulation of biological processes or reactivity associated with solvation/desolvation energies of macromolecules.[20] The reaction equilibrium is affected by changes in the bathing water activity in proportion to the differential hydration between products and reactants.[21] We suggest that a single α-(1→6)-glycosidic linkage in **XAN16** functions as a novel entropic regulator, which reduces the conformational entropy of **XAN16** and increases the motional entropy of solvent water molecules. Our findings provide a molecular interpretation of the hypothesis that symbiotic bacteria regulate water activity using the cyclic OPG to alter the rotational entropy of water molecules. The theoretical finding on a novel entropic regulator described herein could be extended to various other glycosidic linkages in the field of carbohydrate engineering and could also be applied to the area for osmo-regulation of carbohydrates with various linkage patterns.

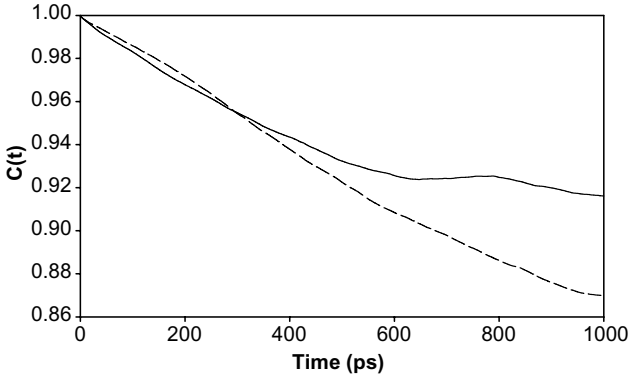

Figure 9. Solvent effects on global solute motion. The normalized autocorrelation functions for vectorial motions are plotted versus time for **XAN16** (solid line) and **CYS16** (dashed line). The vector connected by two glycosidic oxygens between residue **1** and **8** was used in this calculation.

Acknowledgments

This study was supported by a grant from the MIC (Ministry of Information and Communication) through the National Grid Infrastructure Implementation Project of KISTI (Korea Institute of Science and Technology Information) and partially supported by a National R&D project in MOST for Biodiscovery in Korea SDG.

References

1. (a) Matthews, B. W.; Nicholson, H.; Becktel, W. J. *Proc. Natl. Acad. Sci. U.S.A.* **1987**, *84*, 6663–6667; (b) Mainfroid, V.; Mande, S. C.; Hol, W. G. J.; Martial, J. A.; Goraj, K. *Biochemistry* **1996**, *35*, 4110–4117.
2. (a) Wang, G.; Li, S.; Lin, H.; Brumbaugh, E. E.; Huang, C. *J. Biol. Chem.* **1999**, *274*, 12289–12299; (b) Menger, F. M.; Chen, X. Y.; Brocchini, S.; Hopkins, H. P.; Hamilton, D. *J. Am. Chem. Soc.* **1993**, *115*, 6600–6608.
3. Herman, P. S. *Annu. Rev. Microbiol.* **2000**, *54*, 257–268.
4. (a) Cumming, D. A.; Carver, J. P. *Biochemistry* **1987**, *26*, 6664–6676; (b) Woods, R. J. *Glycoconjugate J.* **1998**, *15*, 209–216.
5. (a) Amemura, A.; Cabrera-Crespo, J. *J. Gen. Microbiol.* **1986**, *132*, 2443–2452; (b) Talaga, P.; Stahl, B.; Wieruszeski, J. M.; Hillenkamp, F.; Tsuyumu, S.; Lippens, G.; Bohin, J. P. *J. Bacteriol.* **1996**, *178*, 2263–2271.
6. (a) York, W. S. *Carbohydr. Res.* **1995**, *278*, 205–225; (b) Lippens, G.; Wieruszeski, J. M.; Talaga, P.; Bohin, J. P.; Desvaux, H. *J. Am. Chem. Soc.* **1996**, *118*, 7227–7228; (c) Lippens, G.; Wieruszeski, J. M.; Horvath, D.; Talaga, P.; Bohin, J. P. *J. Am. Chem. Soc.* **1998**, *120*, 170–177.
7. Brooks, B. R.; Bruccoleri, R. E.; Olafson, B. D.; States, D. J.; Swaminathan, S.; Karplus, M. *J. Comput. Chem.* **1983**, *4*, 187–217.
8. Jorgensen, W. L. *J. Chem. Phys.* **1982**, *77*, 4156–4163.
9. Darden, T.; York, D.; Pedersen, L. *J. Chem. Phys.* **1993**, *98*, 10089–10092.
10. Ryckaert, J. P.; Ciccotti, G.; Berendsen, H. J. C. *J. Comput. Phys.* **1977**, *23*, 327–341.
11. Feller, S. E.; Zhang, Y.; Pastor, R. W.; Brooks, B. R. *J. Chem. Phys.* **1995**, *103*, 4613–4621.
12. (a) Huo, S.; Massova, I.; Kollman, P. A. *J. Comput. Chem.* **2002**, *23*, 15–27; (b) Gouda, H.; Kuntz, I. D.; Case, D. A.; Kollman, P. A. *Biopolymers* **2003**, *68*, 16–34.

13. Dowd, M. K.; French, A. D.; Reilly, P. J. *Carbohydr. Res.* **1992**, *233*, 15–34.
14. (a) Wist, J.; Frueh, D.; Tolman, J. R.; Bodenhausen, G. *J. Biomol. NMR* **2004**, *28*, 263–272; (b) Hoch, J. C.; Dobson, C. M.; Karplus, M. *Biochemistry* **1985**, *24*, 3831–3841.
15. Jarvis, M. C. *Carbohydr. Res.* **1994**, *259*, 311–318.
16. Lee, B.; Richards, F. M. *J. Mol. Biol.* **1971**, *55*, 379–400.
17. Naidoo, K. J.; Kuttel, M. *J. Comput. Chem.* **2001**, *22*, 445–456.
18. (a) Johannesson, H.; Halle, B. *J. Am. Chem. Soc.* **1998**, *120*, 6859–6870; (b) Wallqvist, A.; Berne, B. J. *J. Phys. Chem.* **1993**, *97*, 13841–13851.
19. Lazaridis, T.; Paulaitis, M. E. *J. Phys. Chem.* **1994**, *98*, 635–642.
20. Eisenberg, D.; McLachlan, A. D. *Nature* **1986**, *319*, 199–203.
21. (a) Colombo, M. F.; Rau, D. C.; Parsegian, V. A. *Science* **1992**, *256*, 655–659; (b) Parsegian, V. A.; Rand, R. P.; Rau, D. C. *Proc. Natl. Acad. Sci. U.S.A.* **2000**, *97*, 3987–3992.